RSC Advances

ROYAL SOCIETY OF CHEMISTRY

www.rsc.org/advances

Distribution of carbon nanotubes in fresh ordinary Portland cement pastes: understanding from a two-phase perspective

Shu Jian Chen[1], Wei Wang[1], Kwesi Sagoe-Crentsil[2], Frank Collins[1], Xiao Ling Zhao[1], Mainak Majumder[3] and Wen Hui Duan[1]*

[1]Department of Civil Engineering, Monash University, Clayton, VIC, 3800, Australia

[2]CSIRO Manufacturing & Infrastructure Technology, Highett, Victoria 3190, Australia

[3]Department of Mechanical and Aerospace, Monash University, Clayton, VIC, 3800, Australia

Abstract

Significant research advances have been made in the field of carbon nanotube (CNT) reinforced ordinary Portland cement (OPC) paste composites in recent years. However, the distribution of CNTs in fresh OPC paste is yet to be fully researched and quantified, thereby creating a technical barrier to CNT utilization in concrete construction. In this study, fresh OPC paste was treated as a two-phase material containing solid particles (cement grains) and liquid solutions (pore solutions). A centrifugation-based technique was proposed to separate these two phases and the presence of CNTs in each phase was quantified. UV-Vis spectrometry showed that the degree of dispersion can achieve above 90wt% using polycarboxylate superplasticizer. The results suggested an upper limit of 0.26wt% for CNT addition into water before mixing with OPC, and the dispersion was found to be stable for at least 4 hours. Based on scanning electron imaging, the adsorption phenomenon of CNTs on OPC grains with size less than 4 μm was discovered. Energy-dispersive X-ray spectroscopy indicated these adsorptive particles have lower Ca to Si ratio. It was observed that about 0.5 mg of CNTs per gram of OPC grains was adsorbed in solid OPC grains in typical fresh OPC pastes. On the basis of these results, a conceptual model was proposed for the distribution of CNTs in fresh OPC paste where about 33wt% of the CNTs stays in pore solution and 65wt% of CNTs adsorbed on OPC grains

*Corresponding author. E-mail: wenhui.duan@monash.edu (Wen Hui Duan)

Keywords: carbon nanotubes, cement paste, adsorption, centrifuge, UV-vis spectrometry, dispersion.

*Corresponding author. E-mail: wenhui.duan@monash.edu (Wen Hui Duan)

1. Introduction

Carbon nanotube (CNT) reinforced ordinary Portland cement (OPC) composites have attracted considerable attention in recent years. Much research has focused on improving the engineering properties of OPC pastes using CNTs [1-6]. It has been found that the addition of CNTs can improve compressive and flexural strength, fracture toughness, Young's modulus [7], porosity [8], electrical resistance [9], and piezoresistivity [10, 11] of the composite.

All these property modifications using CNTs are affected by the distribution of CNTs in the OPC paste matrix. In order to utilized the superior properties of CNTs such as high strength, high electrical and thermal conductivity and large aspect ratio, it is preferred that the CNTs to be well distributed in the matrix as single-tubes instead of agglomerates[7]. Understanding the distribution of CNTs in OPC paste is essential to study the modification effect of the CNTs.

After mixing with CNT aqueous solution, the OPC powder turns into a paste and the hydration reaction begins. The fresh OPC paste is a fluid before it gradually loses its fluidity due to the reaction. After a period of time, the paste turns into a rigid gel, hardened OPC paste [12]. Correspondingly, three main approaches have been adopted in literature to investigate the dispersion of CNTs: (1) to investigate the dispersion of CNTs in aqueous solutions before mixing [13]; (2) to measure the viscosity of fresh OPC paste [14]; (3) to use the properties of the hardened paste to indicate the effectiveness of the dispersion [14, 15].

The dispersion of CNTs in aqueous solutions has been studied in depth in the past decade. Dispersion using surfactants is often desired as it preserves the integrity of the CNT walls. Unfortunately, many of the popular surfactants for dispersing CNTs in water [16-18] have problems of compatibility with OPC pastes [7]. In the work of Collins et al. [13], where different OPC-compatible surfactants (cement additives) were used to disperse CNTs in water, polycarboxylate-based superplasticizer was found to give the best dispersion results. Studies have also shown that multi-walled CNTs can be dispersed more easily due to their larger diameter [7] compared with single-walled CNTs.

As CNTs have a large specific surface area that absorbs water, studies have generally reported increased viscosity of the fresh paste when CNT is incorporated [7]. It has also been suggested that the CNTs may act as nucleation sites, accelerating the hydration reaction and thereby increasing the viscosity [7, 8, 19]. In the authors' previous study, the viscosity of the fresh paste was found to increase with an increase in the amount of dispersed CNTs in aqueous solutions [14].

Other studies [7, 14, 15] have shown that significant improvement in the mechanical properties of the hardened paste can be achieved by using polycarboxylate superplasticizers as dispersant. These findings suggest that the use of polycarboxylate superplasticizers in collaboration with ultrasonication is one of the most efficient methods for achieving improved mechanical properties of the hardened pastes. Improvement of the mechanical properties of the hardened paste is often taken to imply that the CNTs are well dispersed in CNT-OPC paste composites [7, 13-15].

Although these three approaches have increased understanding of the dispersion of CNTs, they all considered the OPC paste as a single-phase material (either water or paste fluid or hardened solids), which is inadequate to describe CNT distribution. Fresh OPC paste is a complex alkaline environment that contains various types of ions and particles. The particle size ranges from tens of nanometers to hundreds of micrometers. These particles account for a volume fraction about 40% (with water to cement ratio between 0.4 to 0.6) [12]. CNTs can only reside in the other 60% of the volume, that is filled with pore solutions [12]. In other words, the distribution of CNTs is not uniform at sub-millimeter scale. This uneven distribution is a significant characteristic of the composite, especially when the microstructural modification effect of CNTs is considered [1]. However, existing approaches are unable to characterize this uneven distribution of CNTs in such a complex system.

Due to the limitations in these existing approaches, the distribution in the OPC paste cannot be quantified. And there is limited proof in the literature indicating the amount of CNTs that can stay dispersed in either fresh or cured OPC paste. Therefore, the objective of the present study is to quantify and understand the distribution of CNTs in the fresh OPC paste using new approaches.

Quantification of the distribution in fresh paste helps understand of the dispersion in the hardened pastes.

In the present work, for the first time, we considered the fresh OPC paste as a more realistic two-phase system consisting of a solid particle phase and a liquid solution phase. From this two-phase perspective, we suggest that the term "dispersion" can only be used to describe the CNT status in the liquid phase. The term "adsorption" is used here to describe the interaction between CNTs and solid phase (cement grains). The term "distribution" should be used to describe the status of CNTs in the fresh OPC paste system. We propose a new centrifuge-based approach to separate these two phases to allow quantitative investigation of the CNTs in each phase. As an outcome of this novel approach, the phenomenon of CNT adsorption on the solid particle phase of OPC was discovered. This adsorption phenomenon is likely due to electrostatic or van der Waals forces [20] and has not been considered in any previous publications. The amount of adsorbed CNTs is described by a proposed parameter, the adsorption ratio.

In terms of the CNTs dispersion in the liquid phase, the novel approach effectively isolates the liquid solution in the fresh OPC-CNT paste. By characterizing this solution with UV-Vis spectrometry, the first quantification of CNT dispersion in the liquid phase of fresh OPC paste is obtained. Also, the time-dependent stability of CNT dispersion in the liquid phase is studied. The limit of the CNT dispersion prior to mixing with OPC is also investigated.

After quantification of the CNT dispersion and adsorption in these two phases, a conceptual model is proposed to describe the distribution of CNTs in fresh OPC pastes. This model can be used to refine earlier cracking bridging models [21, 22] and to develop microstructural and hydration models [23-26] for CNT-OPC composites. It should be noted that other particulate matrixes such as ceramic and clay [27, 28] may display similar characteristics to those of OPC pastes, so that this model may be applicable to them.

2. Experimental program

2.1 Materials and instrumentation

Multi-walled CNTs (MWCNTs) were purchased from Nanocyl S.A., Sambreville, Belgium. According to the manufacturer's specifications [29] the average diameter of the CNTs was 9.5 nm and the average length of the tubes was 1.5 μm. The product contained less than 5% metal oxide impurities and less than 4% of –COOH functional group. A commercial polycarboxylate-based surfactant containing particular types of polycarboxylate chains that could effectively disperse CNTs [13] was used as the dispersing agent to improve dispersion of the CNTs in water. Type GP OPC, conforming to the requirements of Australian Standard AS 3972, was used in the adsorption test.

Ultrasonication was applied using a Vibra-cell VCX 500 ultrasonicator from Sonics & Materials, Inc. with a net power output of 500 watt at 20 kHz. A Shimadzu UV 4800 UV-Vis photospectrometer was used to characterize the degree of CNT dispersion. A Centrifuge 5702 from Eppendorf was used to centrifuge the fresh CNT-OPC pastes. The dried CNT suspension on silicon wafers was imaged using an FEI Nova NanoSEM™ 450 SEM with an electron diffraction X-ray (EDX) spectrometer.

2.2 Experimental process

One master-batch of CNT suspension was prepared by adding 2.6wt% of MWCNTs and 10.6wt% of the surfactant into distilled water. This surfactant-to-CNT ratio was determined by the authors' earlier work [14]. CNT suspensions with different total CNT mass concentration (C_t) were obtained by diluting the master-batch with distilled water. Dilution factors of 1:1, 1:5, 1:10, 1:20, 1:50, 1:100, and 1:1000 were used to make the C_t equal to 2.6wt%, 0.26wt%, 0.13wt%, 0.053wt%, 0.026wt%, and 0.0026wt%, respectively.

The CNT suspensions with different C_t were then ultrasonicated using the probe sonicator. The intensity and power output of the ultrasonicator were kept at 40% and 40±3 W respectively. When sufficient ultrasonication energy was applied [14, 21], the maximum dispersed CNT concentration (C_d) was achieved and the CNT suspensions were sampled for UV-Vis measurement. At least two

samples were used in each UV-vis measurement and the coefficient of variation is found to be smaller than 3% (at 500 nm) indicating very consistent suspension of CNTs in the solution. Subsequently the ABS at 500 nm was selected to calculate C_d using the Beer-Lambert Law given as:

$$C_d = \frac{A}{\varepsilon l} \quad (1)$$

where $A = \varepsilon C_d l$ is the average absorbance at a specific wavelength and ε is the specific extinction coefficient [30-32], l = 1 cm is the path length of the light through the CNT suspension. To determine ε, the suspension with C_t = 0.0026wt% and surfactant concentration 1wt% was prepared and diluted by factors of 2, 3, 4, and 5. These suspensions were subjected to ultrasonication until their ABS reached the maximum. With such low C_t, sufficient surfactant and ultrasonication, the CNTs in these suspensions were regarded as fully dispersed. ε was then determined by drawing the linear relation between the ABS and C_t of these suspensions, as shown in the supplementary material. ε was found to be 50 ml mg-1cm-1, is slightly higher than the reported values between 41 and 46 ml mg-1cm-1 [30-32].

To test the stability of the CNT suspensions in alkaline environments, a simulated OPC pore solution was prepared with concentrations of the chemicals as shown in Table 1. This composition of the pore solution [33] typically represents the concentration of Na+, K+, Ca2+, SO4-, and OH- ions in early-age (within about 8 hours) concrete [34]. These ions were introduced into the CNT suspensions with different C_t by mixing the suspensions with the simulated pore solution. During mixing the ion concentration was chosen to be above 90% of the concentration in Table 1. ABSs of these CNT suspensions were then measured every hour until 17 hrs after mixing.

Table 1 Concentration of added chemicals in the simulated concrete pore solution

Added compounds	Concentration (g/L)
NaOH	8
KOH	22.4
$CaSO_4$ $2H_2O$	27.6
$Ca(OH)_2$	Sat.

The suspension with C_t = 0.26wt% was used to investigate the adsorption of CNTs on the surface of OPC grains. 2 ml of the suspension was injected into each Falcon centrifuge tube. Then, 0.1 g, 1 g, 2 g, and 4 g of OPC grains were thoroughly mixed with the suspension in four centrifuge tubes for 2 min using a spatula. After mixing, the CNT-OPC mixtures and the CNT suspension (without added OPC grains) were centrifuged with acceleration of 3000 g (g = 9.8m/s^2) for 7.5 minutes. Upon centrifugation, the OPC particles settled to the bottom of the tubes and the CNT suspension was concentrated to form a supernatant as shown in Figure 1. The UV-Vis spectrum of the supernatant was measured and C_d was calculated based on Eq. 1. When x g of OPC grains was mixed with the CNT suspension and then centrifuged, the adsorption ratio of OPC grains was calculated by

$$\text{adsorption ratio} = (C_d(W_{c,0}) - C_d(W_{c,x}))\frac{V}{x} \qquad \textbf{2}$$

where W_c is the weight of the added OPC grains, C_d ($W_{c,0}$) and C_d ($W_{c,x}$) correspond to the C_d in the mixture with 0 g and x g of OPC grains, respectively, and V = 2 ml is the volume of the suspensions.

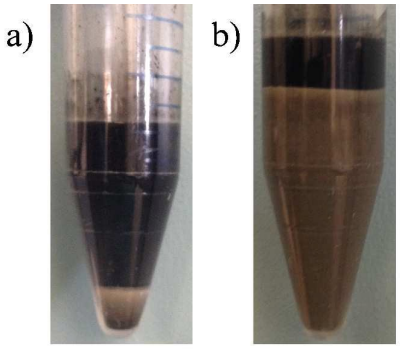

Figure 1. CNT-OPC pastes after centrifugation: (a) 0.1 g and (b) 4 g OPC grains, respectively. The supernatant is the CNT suspension; the grey settlement at the bottom of the tubes is OPC grains.

To examine the morphology of CNTs attached to the OPC grains, the supernatant in the centrifuge tubes was removed by rinsing with ethanol, and then 10 ml of ethanol was added into the tube and mixed with the OPC settlement using a spatula. Mixing with ethanol was essential in order to stop the hydration [12] of the OPC grains so that the adsorbed CNTs would not be covered by

hydration products and would be easily observed under SEM. The ethanol-rinsed particles were then filtered out using grade 1 filter paper. The residue on the filter paper was spread to dry on silicon wafers in a vacuum chamber. After drying in vacuum for 1 week, the residues were attached to carbon tapes and coated with around 2 nm of gold for SEM imaging and EDX spectroscopy measurement. The SEM operated at 5 kV during the imaging and 15 kV during EDX measurement.

3. Dispersion of CNTs in pore solutions

3.1 Dispersion limit of CNTs in aqueous environment

Concentration of dispersed CNTs (C_d) is one of the key factors that influence the reinforcing effect of CNTs. As addressed in the authors' previously proposed model [21], the reinforcing efficiency of CNTs is proportional to the amount of dispersed CNTs in the matrix. Therefore, a higher C_d is desirable for better reinforcing effect. It is well known, however, that CNTs tend to agglomerate in an aqueous environment [16-18, 35, 36], and consequently the C_d is not constantly equal to the dosage of CNTs (C_t) that is the mass ratio between the CNTs and the suspension. Figure 2-a presents the calculated C_d/C_t ratio using Eq. 1 based on UV absorbance of CNT-water suspensions. The C_d/C_t ratio gives an indication of the degree of CNT dispersion in the suspension; a higher C_d/C_t ratio is desirable as it means that more CNTs are in the dispersed state.

Figure 2-a shows that under the ideal dispersion condition, C_d/C_t should reach and stay at 1 when C_t is less than 0.26wt%. $C_t \approx$ 0.13wt% gives the optimal dispersion and $C_t \approx$ 0.26wt% is the maximum dosage that can maintain a high degree of dispersion (>85%). When C_t is greater than 0.53wt% the suspension begins to become saturated with CNTs and the dispersed state of CNTs becomes less energetically feasible [20]. Therefore, C_d/C_t was decreased to less than 40%. In the cases of C_t<0.05wt%, the experimentally measured C_d/C_t dropped to 60-65%. The ideal dispersion, where C_d/C_t remains at 1 when C_t decreases from 0.13wt%, was not achievable under the current experimental conditions because of the fixed surfactant-to-CNT ratio of 4, causing low concentration of the surfactants when C_t<0.05. Consequently, more surfactant dissolved in the solvent as monomers rather than forming an assembly on the CNT surface at low concentration,

thereby decreasing the dispersion efficacy of the surfactant [20, 35, 36]. As demonstrated in Figure 2-a, the data scattering is very small for the UV measurements. Therefore, for clarity and better presentation, the error bars are not presented in Figures 2-b, 3 and 4.

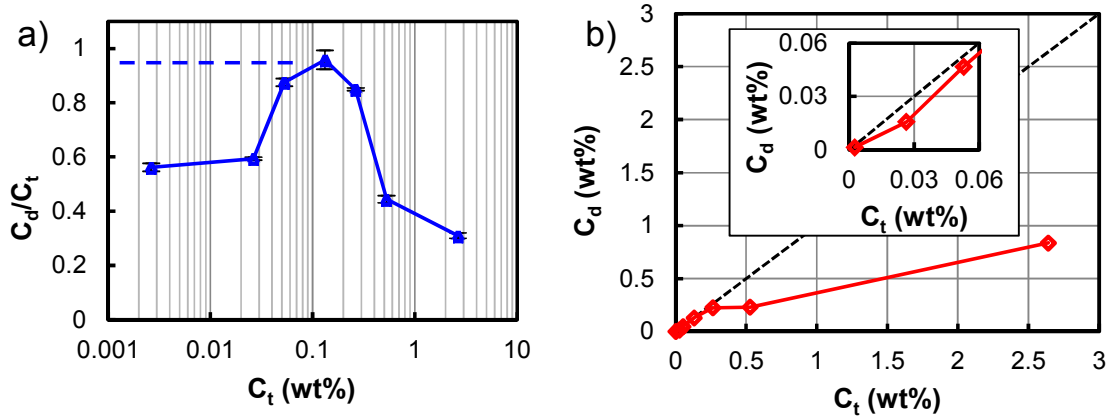

Figure 2. Change in degree of dispersion (C_d/C_t, a) and dispersed CNT concentration (C_d, b) with C_t. The dashed line in (a) shows C_d/C_t under the ideal dispersion condition for ε=50.12 ml/mg/cm. The dashed line in (b) indicates $C_d = C_t$. Insert in (b): zoomed-in view of (b) in the range C_t= 0-0.06. Error bar indicates 1 standard deviation.

Apart from the degree of dispersion (C_d/C_t ratio), the upper limit of C_d is another important parameter for the properties of the composite. Figure 2-b presents the monotonic change of C_d with C_t. The ideal dispersion case is when C_d=C_t (dashed line in Figure 2-b). It can be clearly seen that as C_t increased above 0.26wt%, C_d gained more bias from the C_d=C_t curve, meaning that more CNT agglomerated. It is notable that at very low concentration, as shown in the insert in Figure 2-b, the C_d curve is also slightly biased away from the C_d=C_t curve, which may be due to the detachment of the surfactants. These results show that C_d could rise to around 0.83wt% by increasing C_t to 2.6wt%. The trend of the C_d curve also indicates that C_d may be increased further when C_t exceeds 2.6wt%. However, using such high concentrations would introduce a fair amount of agglomerated CNTs, with possible detrimental effect on the engineering properties of the composite, for example, causing stress concentration.

3.2 Stability of CNTs in alkaline environment

The dispersion of the CNTs presented in Figure 2 was very stable. For example, the C_d/C_t for CNT suspensions decreased by less than 5% after 2 weeks. In contrast, significant changes in C_d/C_t were observed after the simulated pore solution was added into the CNT suspensions. Figure 3 shows the change in C_d/C_t for CNT suspensions with different C_t 18 hours after ultrasonication. It can be seen that C_d/C_t has a decreasing trend in general regardless of C_t. This suggests that the dispersion of CNTs in OPC pore solution is not stable in the long term. However, there is a transition point during the change of C_d/C_t as shown in Figure 3-a. Transition points can be readily identified by the gradient of the curves.

As demonstrated in Figure 3-b, before the transition point, C_d/C_t decreases almost linearly at a low rate (0.7% per hour for C_t = 0.26wt%), whereas after the transition point C_d/C_t decreases sharply in a nonlinear manner. The corresponding times for the transition points were measured for all the curves in Figure 3-a and listed in Table 2. Decreasing rates of C_d/C_t before the transition point were also obtained by linear regression (Table 2 column 4). It is found that the decreasing rate is affected by two factors. The primary factor is the initial degree of dispersion which increases the decreasing rate except for C_t =0.26wt%. Higher degree of dispersion indicates less CNTs are in agglomerated form which are, thermodynamically, more stable than the CNTs in dispersed form [37, 38]. Therefore, higher degree of dispersion with more dispersed CNTs increases the agglomeration rate based on Boltzmann distribution and law of mass action [20]. The second factor is the abundancy of polycarboxylate surfactants in the suspension. Higher concentration of polycarboxylate surfactant enhances the steric repulsion[37] and stability of suspension in alkaline environment[37, 38]. This is the reason for the lower decrease rate of C_t =0.26wt% compared with C_t =0.053wt% since C_t =0.26wt% has 5 times higher concentration of polycarboxylate surfactant than C_t =0.053wt%. Because the rates of decrease of all the suspensions were found to be very low, with the maximum of 1.9 percent per hour, the suspension before the transition point could be treated as stable from a practical point of view. The transition points were found to be greater than at least 4 hours in the range of C_t from 0.026wt% to 2.6wt%. OPC pastes normally set within approximately 3-4 hours,

and therefore short-term stability of CNT suspension within an alkaline environment (before the transition point) is sufficient to maintain good dispersion of CNTs in hardened OPC pastes and to avoid re-agglomeration of the CNTs.

The mechanism behind the transition point is complex. Former studies in flocculation processes in colloid systems containing fibrous particles have also suggested a two-stage flocculation process [39]. The existence of the transition point is related to the agglomeration process of CNTs in the pore environment of OPC pastes. Prior to the transition point, the CNTs tend to form one-dimensional bundles, each of which contains several parallel CNTs, but afbter the transition point these bundles further agglomerate into three-dimensional mesh or cage-like large agglomerates. A detailed explanation with the assistance of molecular dynamics simulations can be found elsewhere [40].

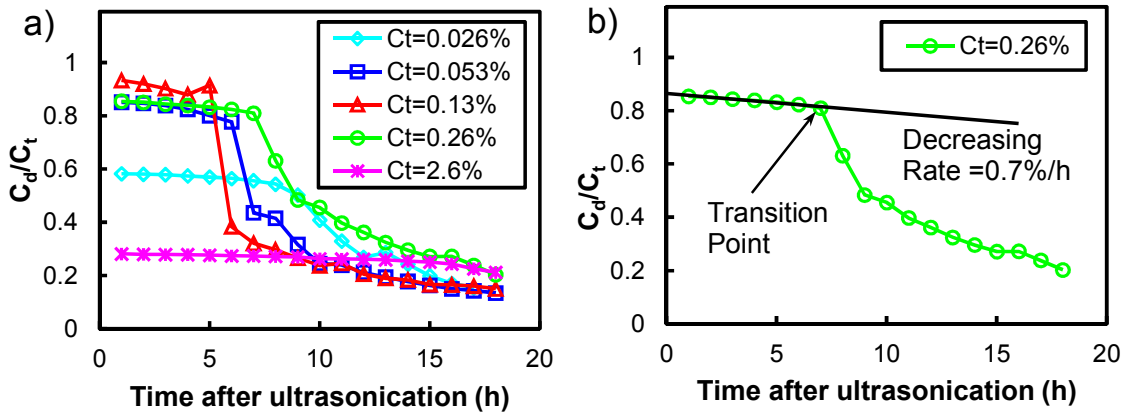

Figure 3. (a) Stability of CNT dispersion in simulated OPC pore solution at different durations after mixing. (b) Determination of the transition point and rate of decrease of C_d/C_t.

Table 2. Transition time in dispersion state

C_d/C_t	Total CNT concentration (C_t,wt%)	Transition point (h)	Rate of decrease of C_d/C_t (%/h)
0.28	2.6	16	0.2
0.58	0.026	8	0.5
0.85	0.053	6	1.6
0.85	0.26	7	0.7
0.93	0.13	4	1.9

4. Adsorption of CNTs on OPC grains

When mixed within OPC pastes, CNTs adsorb on cement grains due to van der Waals or electrostatic forces, as well as dispersing in pore solutions as discussed in section 3. The amount of CNTs adsorbed by OPC grains was measured and is shown in Figure 4.

It can be seen that the CNT adsorption ratio, defined as the amount of CNTs adsorbed per gram of OPC grains, decreased with the cement-to-water ratio (c/w). If a relatively small quantity of OPC (W_c=0.1g, c/w=0.05) was added into the CNT suspension with C_t=0.26wt%, around 2.7 mg of CNTs was adsorbed by 1 g of OPC grains. When c/w rose to 2, the adsorption ratio reduced significantly to 0.51 mg/g. Adding more OPC grains into the suspensions when c/w >1 produced no noticeable change in the adsorption ratios with c/w = 2 (or w/c = 0.5, which is commonly used in cement and concrete composites).

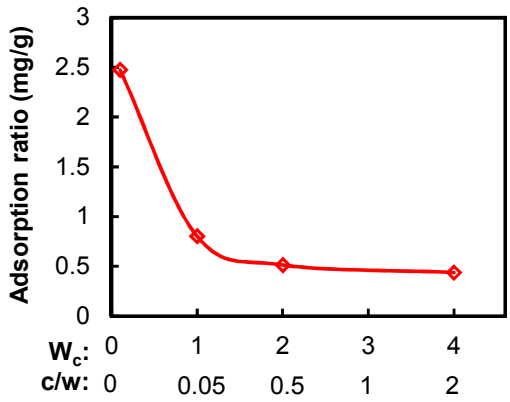

Figure 4. Amount of CNTs adsorbed on cement grains vs the weight of added OPC (W_c) and the cement-to-water ratio (c/w).

SEM images were also taken of OPC pastes with different c/w ratios, as shown in Figure 5. The CNT concentration was fixed at 0.26wt%. Two interesting observations can be made. First, CNT adsorption on OPC grains was selective and preferential to smaller grains (the areas within the yellow dashed lines in Figure 5-a and b). Second, a thick layer of heavily agglomerated CNTs covered the surface of these small OPC grains (Figure 5-a and b) when the amount of added OPC was small (c/w = 0.005 or w/c=200). As shown in Figure 5-c and d, when c/w= 2 (or w/c=0.5), no significantly layer-like agglomeration of CNTs is observed; instead, the CNTs scatter on the OPC

grain surfaces. This reduction in the adsorption ratio and layer thickness of CNTs was attributable to the larger surface area of these small OPC grains as well as the more limited space for CNTs to travel during the adsorption process when the cement-to-water ratio increased.

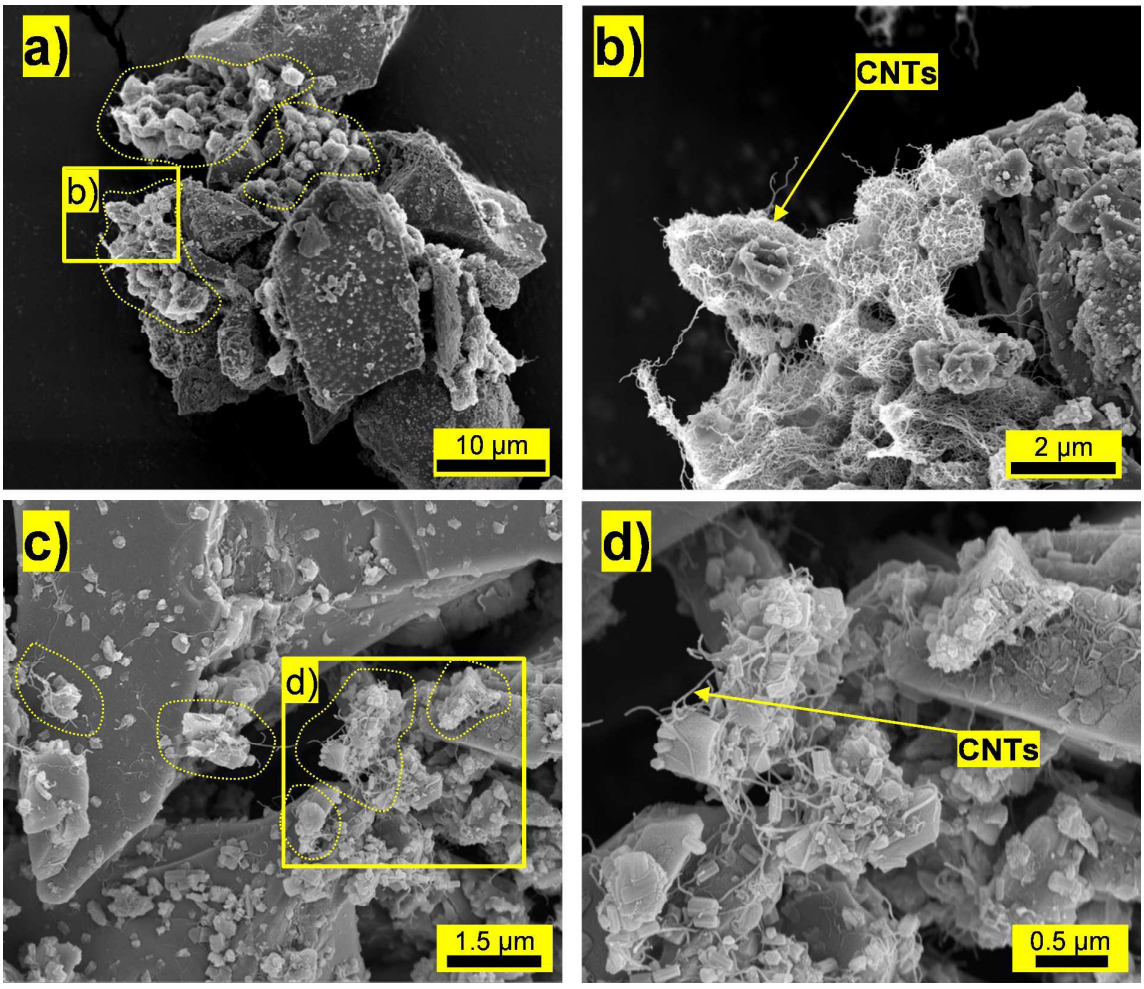

Figure 5. SEM images of OPC particles and CNTs adsorbed on OPC particles. (a & b) with 0.1 gram of OPC and (c & d) with 4 grams of OPC in CNT suspension with C_t= 0.26wt%.

To understand why CNTs preferred smaller OPC grains, the geometry and chemical composition of these OPC grains were examined. The size of these adsorptive OPC grains was measured based on about 20 SEM images. The particle size distribution of these OPC grains is plotted in Figure 6. The measurement shows that about 98% of the adsorptive particles were smaller than 4±0.5 μm (the longest dimension). The major components of OPC grains within this size range were most likely alite or gypsum [12].

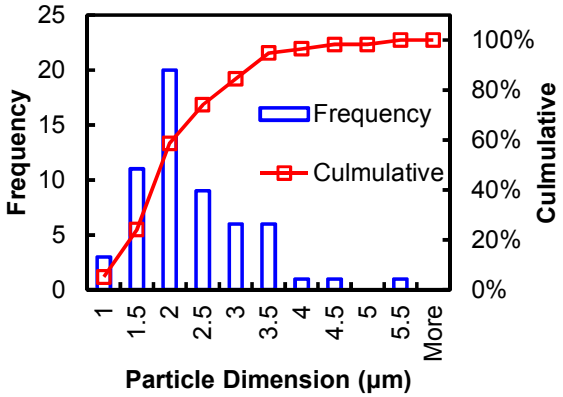

Figure 6. Particle size distribution of the adsorptive OPC particles. The particle dimension measured is the longest dimension of the particle.

Figure 7 shows typical EDX spectra of small (adsorptive) and large (non-adsorptive) OPC grains. Calcium, silica, aluminum and oxygen are detected on both type of grain. Since no sulfur is observed on the spectrum, it is inferred that neither type of grain is likely to be gypsum (Ca_2SO_4), which is a common retarder added into OPC to extend the setting time of OPC pastes [12]. Clearly, a very high carbon peak in the adsorptive (or small) grains was caused by the adsorbed CNTs. Another distinction between the two type of grain is that a much more significant peak of calcium is present for the non-adsorptive (or large) grains. This indicates that the non-adsorptive grains are likely to have a higher Ca/Si ratio than the adsorptive ones. Past research has shown that hydration products have lower Ca/Si ratios (1.6-1.9) [41] than unhydrated cement particles, that are primarily composed of alite and belite with Ca/Si ratio of 3 and 2, respectively [42]. Furthermore, smaller OPC grains have been found to possess less belite than larger grains [42]. Therefore, it was inferred that the smaller (or adsorptive) particles contained a higher fraction of hydration products and less belite.

The reasons why CNTs tended to adsorb on smaller OPC grains can be inferred from the results in Figures 5-7. First of all, the smaller OPC grains (with high fraction of alite) were more active for hydration during the initial hydration reaction [12], leading to more hydration products on them. These hydration products could bond the -COOH group onto the CNT surface [8]. The nucleation effect of the CNTs [7] may also stimulate the growth of hydration products on CNTs near the small OPC grains, causing the CNTs to be precipitated on the OPC grains. Moreover, the geometry of CNTs

also contributed to the adsorption on smaller OPC grains. The CNT length was comparable to that of the small adsorptive OPC grains, resulting in a flocculation effect [39] where the CNT entrapped small OPC grains in the suspension.

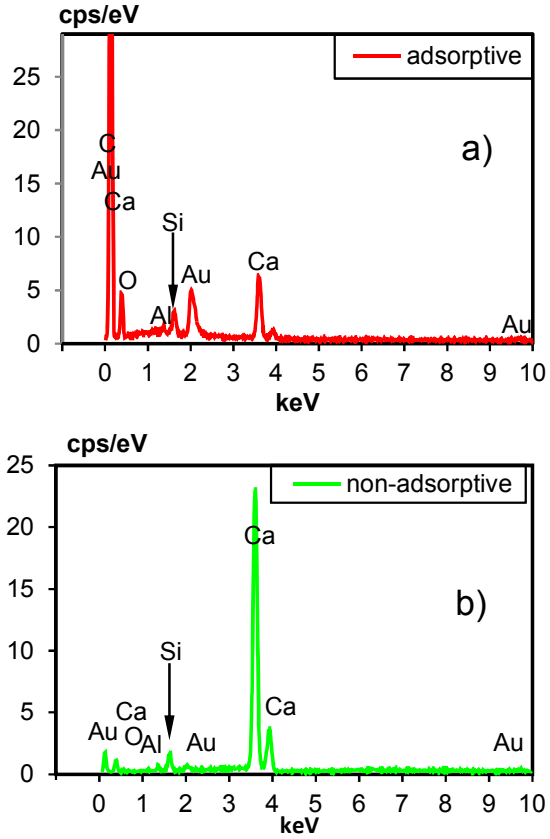

Figure 7. Typical EDX spectra for (a) small particles wrapped by CNTs and (b) larger particles without CNTs.

5. Distribution of CNTs in OPC pastes

As shown on Figure 8, at sub-millimeter scale, CNT distribution was not uniform in the fresh OPC pastes. Around 40% of the space was occupied by OPC grains at a common w/c between 0.4 and 0.6 [12], which would result in some CNT-free zones within hardened OPC pastes, that had been occupied by OPC grains in the fresh pastes. Acknowledgment of this nonuniformity of CNT distribution is critical to the understanding and modelling of hydration, reinforcing effects, and thermal and electrical conductivity of the CNT-OPC composite.

From the discussion in sections 3 and 4, CNTs appeared to have three states in fresh OPC pastes, as shown in Figure 8, namely the agglomerated state (black), the dispersed state (green), and the

adsorbed state (red). Obviously, the heavily agglomerated CNTs had a low aspect ratio and therefore made negligible contribution to the reinforcing effect [21] although they could still act as fillers affecting the hydration and workability of CNT-OPC [14]. The amount of agglomerated CNTs can be estimated from Figure 2. If C_t is at the optimum value of 0.26wt%, the amount of agglomerated CNTs is less than 2% (calculated from $(C_t\text{-}C_d)/\ C_t$) of C_t (Figure 2)).

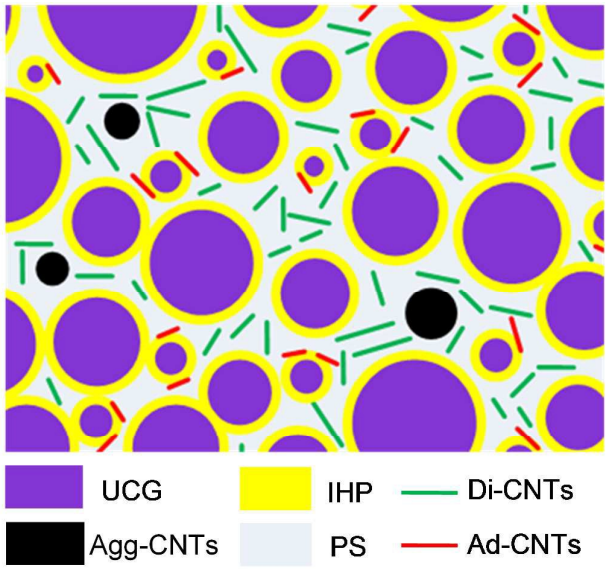

Figure 8. Schematic of the distribution of CNTs in fresh OPC matrix. UCG: unhydrated OPC grains IHP: dydration product formed during initial hydration; Di-CNTs: dispersed CNTs; Agg-CNTs: agglomerated CNTs; PS: OPC pore solution; Ad-CNTs: CNTs adsorbed on small OPC particles.

For a common mix of fresh OPC pastes with w/c ratio of 0.5, the amount of adsorbed CNTs was calculated to be 33% of the C_t in the CNTs suspension with C_t= 0.26wt%. The dispersed CNTs accounted for the remainder (around 65wt%) of the C_t after mixing with OPC. As shown in Figure 5-c and d, with a w/c ratio of 0.5, the adsorbed CNTs do not appear to form dense and thick agglomerations. For further understanding of the effect of the adsorbed CNTs, the surface density of the adsorbed CNTs, which is the number of CNTs attached per unit area of adsorptive OPC grain surface, was estimated using a spherical shape model [12, 43]. The typical particle size distribution function of OPC grains is given by

$$R(d) = \exp\left(-\left(\frac{d}{23.6}\right)^{0.9}\right) \qquad 3$$

where R is the mass fraction of the grains with diameter greater than d [44]. Eq. 3 with the two parameters (23 and 0.9) is a widely used empirical representation of the particle size distribution of OPC [44]. Based on Eq. 3, the total surface area for particles with a certain size can be calculated by [12]

$$S(d) = 6\times10^{6}\times F\times\frac{\mathrm{d}R}{\mathrm{d}d}\frac{1}{\rho d} \quad (4)$$

where $S(d)$ is the surface area of particles with diameter equal to d, F (typically equaling 1.1) is an empirical constant taking into account the shape of the particles, ρ = 3.2 is specific gravity of the OPC grains [12].

The total surface area of the OPC grains with diameter less than 4 μm (s_4) was calculated as 0.28 m^2/g using

$$s_4 = 6\times10^{6}\times F\times(1-R(2))\frac{1}{\rho}+\int_{x=2}^{x=4} S\,\mathrm{d}(d) \quad (5)$$

where, in order to obtain a realistic surface area estimation that matched the observed results [12], OPC grains smaller than 2 μm were assumed to have an average diameter of 1 μm and their surface area was calculated by $6\times10^{6}\times F\times(1-R(2))\rho$ and for 4 μm ≥ d ≥ 2 μm, and the surface area was calculated as an integration of S. [12]. Excluding the 15% contribution to surface area from gypsum [12], the adsorptive area was 0.24 m^2/g (0.28 −0.28 ×15% = 0.24 m^2/g). The adsorptive area (0.24 m^2/g) is around 60% of the total surface area (0.4 m^2/g from Eq 4) of the OPC grains.

Assuming that CNTs are cylinders, the mass of a single multi-walled CNT could be calculated as

$$M_t = \rho_{CNT} L_{CNT}\pi\frac{d^2{}_{CNT}}{4} \quad (6)$$

where ρ_{CNT} is the specific gravity of CNTs, which was adopted as 2.6 g/cm^3 [45], the diameter (d_{CNT}) and length (L_{CNT}) of the CNTs were adopted as 9.5 nm and 1-2 μm based on the measurement in Chen's previous study [21]. As a result, the mass of a single tube (M_t) was computed as 1.8×10^{-16}-3.7×10^{-16}g.

The surface density of CNTs was calculated as

$$\text{surface density} = \frac{\text{adsorption rate}}{s_4 M_t} \quad (7)$$

For the case of c/w = 20 and 2 (with adsorption ratios of 2.5 and 0.44 mg/g respectively), the surface density was found to be 28-56 and 5-10 tubes/μm^2, respectively. These calculated surface densities coincided with the SEM observation in Figure 5, which also proved that the reduction of C_d in paste was mainly due to adsorption rather than agglomeration.

For the common OPC mix with c/w=2 (or w/c=0.5), the surface density of 5-10 tubes/μm^2 corresponded to a thin layer of scattered CNTs on small OPC grains (Figure 5-c, d). However, this surface density was still far higher than the projected surface density of dispersed CNTs that was obtained by evenly splitting the number of CNTs in a 1 μm cubic space into its 6 facets as 65% C_t /M_t/6 =0.8-1.8 tubes/ μm^2. It is suggested here that the adsorbed CNTs distributed more densely than the dispersed CNTs but less densely than the CNT agglomerates. The distribution model of CNTs within OPC pastes is meaningful for understanding of the role of CNTs with regard to reinforcement [14, 21]. Moreover, it is vital for simulating hydration reactions in OPC [23-25] as it allows establishment of the initial particle packing model for fresh paste.

The quantification of CNT adsorption and dispersion in the fresh OPC paste also gives indications on the distribution of CNTs in hardened OPC paste. Due to the strong attraction between CNT and adsorptive OPC grains [20], the adsorbed CNTs is likely to stay on the OPC grains during hydration. Based on section 3.2, the dispersed CNTs in the pore solutions may stay dispersed for a few hours if undisturbed. Considering the hydration products may grow on the CNTs [19] during hydration reaction, these hydration products separate individual CNTs and help resisting the agglomeration of CNTs.

The authors' previous study[14] on cured OPC paste indicates that adding 0.08 wt% (of cement powder) of CNTs into OPC paste significantly increases the flexural strength and fracture energy of the composite for more than 50 % while more than 1wt% of traditional fibers [46] is require to achieve such improvements. This is in agreement with the superior reinforcing potential of CNTs suggested

by the crack bridging models [21, 22]. The reinforcing effect was found to be proportional with C_t when C_t is increase from 0.09 wt% to 0.19 wt%[14]. This proportional relationship only exists when most of the CNTs are effectively separated in the cured matrix as suggested by the authors' crack bridging model for CNTs[21]. These reinforcing effects on cured paste agrees with distribution of CNTs shown in this study where most (above 90 wt%) of the CNTs can stay in pore water or attached to small cement particles that contributes to the separation of CNTs in cured paste. Coinciding with the fiber crack-bridging theories [21, 22], these results show the linear relationship between amount of separated CNTs in fresh paste and the reinforcing effect of CNTs in cured paste.

It should be noted that OPC pastes are very complex mixtures in nature. The conceptual model for typical fresh CNT-OPC paste proposed herein represents the very early stage of the composite mixture. At this early stage, the paste is assumed to be in two phases, the liquid phase with dispersed CNTs and the solid phase with dispersed CNTs. The experimental techniques developed in this study are also applicable to other CNT-OPC paste fabrication schemes involving different types of cement, CNT, or surfactants.

6. Conclusions

To resolve the question regarding the maximum amount of CNTs that can be dispersed in fresh pastes, a two-step investigation was conducted. The first step determined the maximum C_d in CNT-water suspension before mixing with cement. It was found that the C_d kept increasing with C_t to 0.84wt% when C_t = 2.6wt%. However, the degree of dispersion C_d/C_t dropped sharply to less than 50% when C_t exceeded 0.26wt%, resulting in a significant amount of CNT agglomeration. It is suggested, therefore, that the upper limit for economical and effective use of CNTs is C_t =0.26wt% with a C_d/C_t around 90%. The second step was to examine the stability of the CNT dispersions with different C_t in a simulated pore solution that represented the concentration of most ions in fresh OPC pastes. The results showed that the decrease in C_d/C_t for different C_t was less than 2% per hour for at least 4 hours, indicating that the suspensions were stable within the common setting time of

OPC pastes. After 4–16 hours, however, the suspensions transited into an unstable state and C_d/C_t began to decrease drastically.

In terms of CNT distribution in cement paste, there are two major findings in this study. Firstly, the existence of CNT-free zones in the CNT-OPC composite was addressed here in CNT distribution models, where the CNT-free zones were caused by unhydrated grains in the fresh OPC paste. Secondly, the adsorption effect of the OPC grains was proposed and quantified based on an innovative centrifuge-based technique. It was observed that for common w/c ratios, about 0.44 mg of CNT was adsorbed by 1 g of cement. This observation was quantified by SEM imaging demonstrating that only non-gypsum OPC grains < 4 μm in size could adsorb the CNTs, due to the formation of hydration reaction products around these small OPC grains.

Combining these findings, a conceptual distribution model for CNTs in OPC is proposed. The model provides a quantification of the amount of dispersed, agglomerated, and adsorbed CNTs in the matrix. The surface density of the adsorbed CNTs is also calculated as 6-11 CNTs per square micrometer. This model can serve as a starting point for establishing or refining models depicting the effect of CNTs on reinforcement and hydration in CNT-OPC composites.

Acknowledgment

The authors are grateful for the financial support of the Australian Research Council in conducting this study. The authors acknowledge the use of facilities within the Monash Centre for Electron Microscopy.

References

1. G. Y. Li, P. M. Wang and X. H. Zhao, *Carbon*, 2005, **43**, 1239-1245.
2. A. Cwirzen, in *Multi-Functional Materials and Structures Iii, Pts 1 and 2*, 2010, vol. 123-125, pp. 639-642.
3. M. S. Konsta-Gdoutos, Z. S. Metaxa and S. P. Shah, *Cement and Concrete Composites*, 2010, **32**, 110-115.
4. J. Luo, Z. Duan, T. Zhao and Q. Li, *Advanced Materials Research*, 2011, **146**, 581-584.
5. S. Musso, J.-M. Tulliani, G. Ferro and A. Tagliaferro, *Composites Science and Technology*, 2009, **69**, 1985-1990.
6. K. Wille and K. Loh, *Transportation Research Record: Journal of the Transportation Research Board*, 2010, **2142**, 119-126.

7. S. Chen, F. Collins, A. Macleod, Z. Pan, W. Duan and C. Wang, *The IES Journal Part A: Civil & Structural Engineering*, 2011, **4**, 254-265.
8. G. Y. Li, P. M. Wang and X. Zhao, *Carbon*, 2005, **43**, 1239-1245.
9. S. Wansom, N. Kidner, L. Woo and T. Mason, *Cement and Concrete Composites*, 2006, **28**, 509-519.
10. G. Y. Li, P. M. Wang and X. Zhao, *Cement and Concrete Composites*, 2007, **29**, 377-382.
11. Y. Xun and K. Eil, *Smart Materials and Structures*, 2009, **18**, 055010.
12. H. F. Taylor, *Cement chemistry*, Thomas Telford, 1997.
13. F. Collins, J. Lambert and W. H. Duan, *Cement and Concrete Composites*, 2012, **34**, 201-207.
14. B. Zou, S. J. Chen, A. H. Korayem, F. Collins, C. Wang and W. H. Duan, *Carbon*, 2015.
15. M. S. Konsta-Gdoutos, Z. S. Metaxa and S. P. Shah, *Cement and Concrete Research*, 2010, **40**, 1052-1059.
16. J. U. Lee, J. Huh, K. H. Kim, C. Park and W. H. Jo, *Carbon*, 2007, **45**, 1051-1057.
17. M. Zhang, L. Su and L. Mao, *Carbon*, 2006, **44**, 276-283.
18. B. Krause, G. Petzold, S. Pegel and P. Pötschke, *Carbon*, 2009, **47**, 602-612.
19. J. M. Makar and G. W. Chan, *Journal of the American Ceramic Society*, 2009, **92**, 1303-1310.
20. J. N. Israelachvili, *Intermolecular and surface forces: revised third edition*, Academic press, 2011.
21. S. J. Chen, B. Zou, F. Collins, X. L. Zhao, M. Majumber and W. H. Duan, *Carbon*, 2014, **77**, 1-10.
22. V. C. Li, *Journal of Materials in Civil Engineering*, 1992, **4**, 41-57.
23. G. Ye, *Experimental study and numerical simulation of the development of the microstructure and permeability of cementitious materials*, TU Delft, Delft University of Technology, 2003.
24. O. Bernard, F.-J. Ulm and E. Lemarchand, *Cement and Concrete Research*, 2003, **33**, 1293-1309.
25. E. Garboczi and D. Bentz, *Cement and Concrete Research*, 2001, **31**, 1501-1514.
26. G. Ye, P. Lura and v. K. van Breugel, *Materials and Structures*, 2006, **39**, 877-885.
27. A. A. White, S. M. Best and I. A. Kinloch, *International Journal of Applied Ceramic Technology*, 2007, **4**, 1-13.
28. H. H. Lee, U. Sang Shin, J. H. Lee and H. W. Kim, *Journal of Biomedical Materials Research Part B: Applied Biomaterials*, 2011, **98**, 246-254.
29. Nanocyl, *Journal*, 2009.
30. Z. Li, G. Luo, W. Zhou, F. Wei, R. Xiang and Y. Liu, *Nanotechnology*, 2006, **17**, 3692.
31. M. D. Clark and R. Krishnamoorti, *The Journal of Physical Chemistry C*, 2009, **113**, 20861-20868.
32. D. Baskaran, J. W. Mays and M. S. Bratcher, *Chemistry of Materials*, 2005, **17**, 3389-3397.
33. P. Ghods, O. Isgor, G. McRae and T. Miller, *Cement and Concrete Composites*, 2009, **31**, 2-11.
34. F. Rajabipour, G. Sant and J. Weiss, *Cement and Concrete Research*, 2008, **38**, 606-615.
35. A. J. Blanch, C. E. Lenehan and J. S. Quinton, *The Journal of Physical Chemistry B*, 2010, **114**, 9805-9811.
36. A. J. Blanch, C. E. Lenehan and J. S. Quinton, *Carbon*, 2011, **49**, 5213-5228.
37. C.-Z. Li, N.-Q. Feng and R.-J. Chen, *Cement and Concrete Research*, 2005, **35**, 867-873.
38. T. Nawa, *Journal of Advanced Concrete Technology*, 2006, **4**, 225-232.
39. J. Buffle and G. Leppard, *Environmental science & technology*, 1995, **29**, 2169-2175.
40. S. J. Chen, B. Zou, F. Collins, X. L. Zhao, M. Majumber, C. M. Wang and W. H. Duan, unpublished.
41. I. Richardson and G. Groves, *Journal of Materials Science*, 1993, **28**, 265-277.
42. M. Gougar, B. Scheetz and D. Roy, *Waste Management*, 1996, **16**, 295-303.

43. J. Sanahuja, L. Dormieux and G. Chanvillard, *Cement and Concrete Research*, 2007, **37**, 1427-1439.
44. B. Osbaeck and V. Johansen, *Journal of the American Ceramic Society*, 1989, **72**, 197-201.
45. Y. J. Hwang, Y. C. Ahn, H. S. Shin, C. G. Lee, G. T. Kim, H. S. Park and J. K. Lee, *Current Applied Physics*, 2006, **6**, 1068-1071.
46. A. Bentur and S. Mindess, *Fibre reinforced cementitious composites*, CRC Press, 2006.

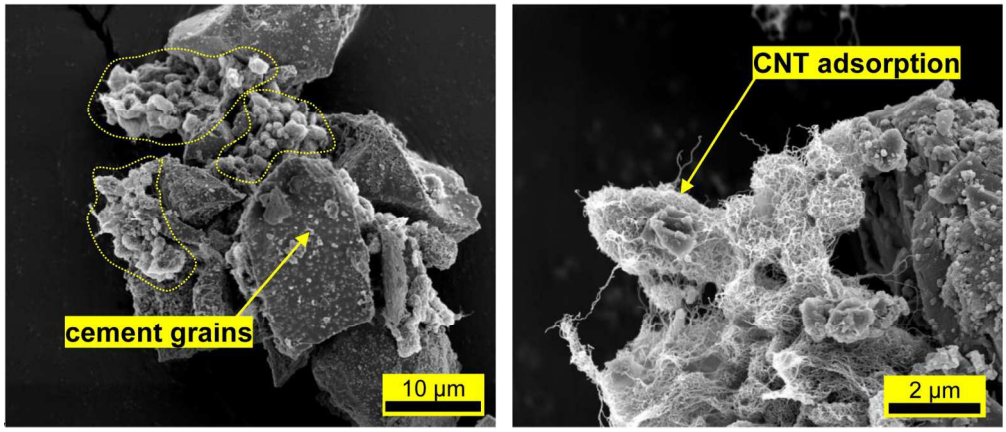

153x65mm (300 x 300 DPI)